Author Manuscript Published OnlineFirst on August 9, 2018; DOI: 10.1158/1078-0432.CCR-18-0862
Author manuscripts have been peer reviewed and accepted for publication but have not yet been edited.

Single Cell Analyses of Prostate Cancer Liquid Biopsies Acquired by Apheresis

Maryou B. Lambros[1*], George Seed[1*], Semini Sumanasuriya[1,2*], Veronica Gil[1], Mateus Crespo[1], Mariane Fontes[2], Rob Chandler[2], Niven Mehra[1,2], Gemma Fowler[1], Berni Ebbs[1], Penny Flohr[1], Susana Miranda[1], Wei Yuan[1], Alan Mackay[3], Ana Ferreira[1], Rita Pereira[1], Claudia Bertan[1], Ines Figueiredo[1], Ruth Riisnaes[1], Daniel Nava Rodrigues[1], Adam Sharp[1,2], Jane Goodall[1], Gunther Boysen[1], Suzanne Carreira[1], Diletta Bianchini[2], Pasquale Rescigno[1,2], Zafeiris Zafeiriou[1,2], Joanne Hunt[2], Deirdre Moloney[2], Lucy Hamilton[2], Rui P. Neves[4], Joost Swennenhuis[5], Kiki Andree[5], Nikolas H. Stoecklein**[4], Leon W.M.M. Terstappen**[5], Johann S. de Bono** [1,2]

* Co-first authors
** Co-senior authors
Corresponding author

Affiliations:
1- Division of Clinical Studies, The Institute of Cancer Research, London, UK
2- The Royal Marsden NHS Foundation Trust, London, UK
3- Divisions of Molecular Pathology and Cancer Therapeutics, The Institute of Cancer Research, London, UK
4- Department of General, Visceral and Pediatric Surgery, University Hospital of the Heinrich-Heine-University Düsseldorf, Düsseldorf, Germany
5- Department of Medical Cell BioPhysics, University of Twente, Enschede, The Netherlands

Corresponding Author:
Johann de Bono
The Institute of Cancer Research
15 Cotswold Road, London SM2 5NG, United Kingdom
Tel: +44 2087224029
E-mail: Johann.de-Bono@icr.ac.uk

Word count: 3745

Disclosure and Potential conflicts of interest

J.S. de Bono has served as a consultant/advisory board member for Terumo (unpaid) and Menarini (paid). No other potential conflicts of interest were disclosed by the other authors.

Downloaded from clincancerres.aacrjournals.org on April 24, 2019. © 2018 American Association for Cancer Research.

Author Manuscript Published OnlineFirst on August 9, 2018; DOI: 10.1158/1078-0432.CCR-18-0862
Author manuscripts have been peer reviewed and accepted for publication but have not yet been edited.

Abstract

Purpose: Circulating tumor cells (CTCs) have clinical relevance, but their study has been limited by their low frequency. **Experimental Design:** We evaluated liquid biopsies by apheresis to increase CTC yield from patients suffering from metastatic prostate cancer, allow precise gene copy number calls, and study disease heterogeneity. **Results:** Apheresis was well-tolerated and allowed the separation of large numbers of CTCs; the average CTC yield from 7.5mls of peripheral blood was 167 CTCs, whereas the average CTC yield per apheresis (mean volume: 59.5mls) was 12546 CTCs. Purified single CTCs could be isolated from apheresis product by FACS sorting; copy number aberration (CNA) profiles of 185 single CTCs from 14 patients revealed the genomic landscape of lethal prostate cancer and identified complex intra-patient, inter-cell, genomic heterogeneity missed on bulk biopsy analyses. **Conclusions:** Apheresis facilitated the capture of large numbers of CTCs non-invasively with minimal morbidity and allowed the deconvolution of intra-patient heterogeneity and clonal evolution.

Downloaded from clincancerres.aacrjournals.org on April 24, 2019. © 2018 American Association for Cancer Research.

Author Manuscript Published OnlineFirst on August 9, 2018; DOI: 10.1158/1078-0432.CCR-18-0862
Author manuscripts have been peer reviewed and accepted for publication but have not yet been edited.

Statement of Significance:

Apheresis is well-tolerated and is a non-invasive alternative to tumor tissue biopsies, substantially increasing circulating tumor cell yields and allowing the study of tumor evolution and intra-patient heterogeneity during treatment. Serial, repeated, apheresis can interrogate disease evolution, drive key therapeutic decisions and transform prostate cancer drug development.

Downloaded from clincancerres.aacrjournals.org on April 24, 2019. © 2018 American Association for Cancer Research.

Author Manuscript Published OnlineFirst on August 9, 2018; DOI: 10.1158/1078-0432.CCR-18-0862
Author manuscripts have been peer reviewed and accepted for publication but have not yet been edited.

Introduction:

Prostate cancer (PC) remains a major cause of male cancer-related deaths [1]. Studies elucidating disease biology are restricted by poor preclinical models and difficulty acquiring metastatic castration resistant prostate cancer (mCRPC) biopsies [2]. The genomic landscape of both localized and advanced PC has been recently described but bulk tumor biopsy genomics only provide a snapshot of the disease landscape [3]. Moreover, concerns have been raised regarding the ability of bulk biopsy sequencing to document intra-tumor heterogeneity and clonal evolution. Serial biopsies are necessary to evaluate changes imposed by therapeutic selective pressures over time, but their acquisition is challenging, invasive and often not feasible. Less invasive alternatives ("liquid biopsies") could be hugely impactful, allowing serial evaluation, and detecting disease evolution that can influence treatment choices.

Two main forms of liquid biopsy have emerged: Circulating plasma cell-free DNA (cfDNA) and circulating tumor cell (CTC) analyses. Whilst measuring cfDNA concentrations has utility [4], limitations in qualitative analyses deconvoluting intra-patient heterogeneity and accurate calling of copy number aberrations (CNAs), especially deletions, have been acknowledged [5]. CTCs, shed from solid tumors [6] and found in the peripheral blood (PB) of patients with both non-metastatic (5-24%) and metastatic (26-49%) disease [7, 8], can allow the early detection of disease dissemination, prognostication and benefit from therapy [9, 10]. Indeed, CTC evaluation may be superior to radiological assessment in determining response to treatment and outcome. [11-13]

CTC studies can allow non-invasive, serial, tumor genomic characterization during treatment, but a major challenge to this has been their detection in significant numbers to enable genomic, transcriptomic and protein analyses. To overcome these limitations, apheresis has been suggested to increase CTC yield [14]. Apheresis allows processing of the whole blood volume by centrifugation, separating blood components (e.g. red cells, platelets and leukocytes) based on density. Apheresis has a therapeutic role in the management of hematological disorders and is well tolerated with few safety concerns [15]. Previous studies have suggested that CTCs can be collected from apheresis product from patients with and without metastases [14, 16, 17]. CTCs can have a similar density to mononuclear cells and apheresis can increase CTC separation from a larger volume of processed blood. We hypothesized that apheresis, followed by CTC enrichment methods, could allow the safe acquisition of large

Downloaded from clincancerres.aacrjournals.org on April 24, 2019. © 2018 American Association for Cancer Research.

Author Manuscript Published OnlineFirst on August 9, 2018; DOI: 10.1158/1078-0432.CCR-18-0862
Author manuscripts have been peer reviewed and accepted for publication but have not yet been edited.

numbers of viable and intact purified CTC populations from patients with advanced PC, permitting a true liquid biopsy and tumor molecular characterization.

Materials and Methods:

Patient selection and clinical assessment

Eligible patients had histologically confirmed mCRPC. Additional eligibility criteria included: Detectable peripheral blood CTCs (CellSearch™), good bilateral antecubital fossa venous access and no coagulopathy. Clinical assessments included medical history and physical examination, full blood count, biochemical tests and coagulation. Safety assessments were done during apheresis and after 30-days. All patients provided written informed consent. The study was conducted in accordance with the Declaration of Helsinki, with the ethics committee of the Royal Marsden and The Institute of Cancer Research approving the study.

Apheresis (method and CTC detection)

Apheresis was performed using a Spectra Optia™ Apheresis System (Terumo, BCT, Lakewood, CO). Patients were connected to this via two peripheral venous catheters in each cubital vein. Whole blood was anticoagulated before entering the rotating centrifuge. Heavier blood elements including erythrocytes migrated to the outside of the channel, plasma to the centre, and the buffy coat (including mononuclear cells and CTCs) to the middle. The mononuclear cell layer was removed and the remaining blood cells and plasma were constantly returned to the patient to the contralateral arm. Granulocyte-colony stimulating factor was not used. Blood was anticoagulated with citrate dextrose solution A (2-4 500mL infusion bags were required for each procedure).

CTC Enumeration using CellSearch® platform

CTC counts were determined in 7.5mL of PB drawn immediately before, and after, the apheresis; an aliquot of apheresis product containing $200x10^6$ WBC was transferred to a CellSave preservative tube (Menarini, Silicon Biosystems) and mixed with CellSearch™ dilution buffer to a final volume of 8mL. All samples were processed within 96-hours and CTC counts determined by CellSearch® (Menarini, Silicon Biosystems). Briefly, cells were subjected to immunomagnetic capture using anti-EpCAM antibodies and stained with antibodies specific for cytokeratin 8, 18 and 19 (CK-PE), CD45 (CD45-APC) and nucleic acid dye (DAPI). Cells were defined as CTCs when positive for cytokeratin and DAPI and negative for CD45. Images were captured

Downloaded from clincancerres.aacrjournals.org on April 24, 2019. © 2018 American Association for Cancer Research.

Author Manuscript Published OnlineFirst on August 9, 2018; DOI: 10.1158/1078-0432.CCR-18-0862
Author manuscripts have been peer reviewed and accepted for publication but have not yet been edited.

using the CellTracks Analyzer II® (Menarini, Silicon Biosystems) and manually examined to determine the presence of CTC. CellSearch Cartridges were stored in the dark at 4°C before further analyses.

Single cell isolation and amplification

CellSearch cartridge contents were transferred into fresh Eppendorf tubes, washed twice with 150**µ**l of phosphate buffered saline, and FACS sorted (FACS Aria III; Becton, Dickinson and Company) to single CTCs (DAPI+, CK+, CD45-) or WBC (DAPI+, CD45+, CK-). Sorted single CTC or WBC were whole genome amplified (WGA) using Ampli1™ (Menarini, Silicon Biosystems) according to the manufacturer instructions with minor modifications. Cells were lysed, digested for 30-minutes, adaptor ligated for 3-hours and PCR-amplified. The WGA DNA was purified (MinElute™ PCR Purification Kit (Qiagen), quantified using Qubit™ (Invitrogen), and stored at -20□C.

DNA from biopsies

DNA from formalin fixed paraffin embedded (FFPE) biopsies was extracted using the QIAamp™ DNA FFPE Tissue kit (Qiagen), quantified using Qubit™ (Invitrogen), and evaluated by Illumina FFPE QC kit™. Whole genome amplification was carried out on 10ng of tumor DNA using WGA2™ (Sigma Aldrich). WGA DNA was purified (MinElute PCR Purification Kit; Qiagen), quantified (Qubit; Invitrogen), and stored at -20□C.

Array Comparative Genomic Hybridization (aCGH)

500ng of amplified single CTC DNA was fluorescently labeled with Cy5, and WBC reference DNA labeled with Cy3 (SureTag Complete DNA Labeling Kit; Agilent Technologies CA, USA). Labeled DNA was purified and hybridized utilizing the Agilent SurePrint G3 Human array CGH Microarray Kit, 4x180K. Slides were scanned and ratios of CTC/WBC determined using CytoGenomics Software v 4.0.3.12 (Agilent Technologies CA, USA). Log_2 ratios of aCGH segments were matched with gene coordinates to assign per-gene values. Copy states of genes were classified by the assigned log_2 ratio values. Log_2 ratio values < −0.25 were categorized as losses; those > 0.25 as gains; and those in between as unchanged. Amplifications were defined as smoothed log_2 ratio values ≥1.2 and homozygous deletions as the segment log_2 ratio values ≤ -1.2.

Per-sample CNA burden was calculated as the proportion of the human genome (3000 Mega-base pairs) impacted. Unsupervised hierarchical clustering was performed using

Downloaded from clincancerres.aacrjournals.org on April 24, 2019. © 2018 American Association for Cancer Research.

Author Manuscript Published OnlineFirst on August 9, 2018; DOI: 10.1158/1078-0432.CCR-18-0862
Author manuscripts have been peer reviewed and accepted for publication but have not yet been edited.

R (v3.4) with Ward's method and the Euclidean distances of unique copy number changes. When clustering samples from multiple tissue types, X chromosome genes were excluded (aside from the *AR* gene and ten genes on either side) due to different reference X-chromosome ploidies (as a female reference was used). Per-patient functional diversity was derived from cluster dendrograms of CTC samples by calculating the sum of connecting branches in a dendrogram (from the R package vegan v2.4.4) and divided by the number of samples.

FISH analysis

FISH was performed by FFPE hybridization as previously described [22]. Briefly 3-4μM FFPE sections were deparaffinized, heat pre-treated, pepsin digested and hybridized with FISH probe hybridization mix overnight at 37^0C. FISH probes used were: BRCA2/CEN13q (Abnova); RB1 (Abbott Laboratories); PTEN (10q23)/SE 10; MYC (8q24)/SE 8 (Leica Microsystems) and a custom-made AR/CEPX probe (Menarini, Silicon Biosystems). Stringency washes were performed on all slides; for AR, where the probe was indirectly labelled, a secondary incubation with anti-Digoxigenin-Fluorescein antibody (Roche Diagnostics, USA) was done. Slides were digitally imaged (Bioview Ltd., Rehovot, Israel) and a pathologist (DNR) evaluated a minimum of 100 tumor cells; the ratios between probes of interest and reference probes were recorded. Amplification was reported if the ratio was >2; heterozygous loss and homozygous deletion if at least 1/3 of the cells showed loss of one copy, or loss of all copies, of the tested probe respectively.

Organoid culture

For CTC enrichment, 1ml of single cell suspension was immunomagnetically separated with EasySep™ Epcam positive selection (Stem Cell Technologies) and the selected fraction used for organoid culture (negative fraction cultured as a control). Isolated cells were seeded in 3D using growth factor reduced Matrigel™ (Corning) in spheroid-forming suspension in ultra-low attachment surface-coated microplates (Nunclon Sphera™, ThermoFisher Scientific) utilizing previously described growth media conditions [23]. Organoids were passaged after 4-6 weeks and cells collected manually for molecular studies by dissociation with TrypLE (Sigma-Aldrich) for 5 min at 37°C.

Next generation sequencing

Downloaded from clincancerres.aacrjournals.org on April 24, 2019. © 2018 American Association for Cancer Research.

Author Manuscript Published OnlineFirst on August 9, 2018; DOI: 10.1158/1078-0432.CCR-18-0862
Author manuscripts have been peer reviewed and accepted for publication but have not yet been edited.

Whole exome sequencing (WES) was performed using Kapa Hyper Plus library prep kits and the Agilent SureSelectXT V6 target enrichment system. Paired-end sequencing was performed using the NextSeq™ 500 (2x150 cycles; Illumina). FASTQ files were generated from the sequencer's output using Illumina bcl2fastq2 software (v.2.17.1.14, Illumina) with the default chastity filter to select sequence reads for subsequent analysis. All sequencing reads were aligned to the human genome reference sequence (GRCh37) using the BWA (v. 0.7.12) MEM algorithm, with indels being realigned using the Stampy (v.1.0.28) package. Picard-tools (v.2.1.0) were used to remove PCR duplicates and to calculate sequencing metrics for QC check. The Genome Analysis Toolkit (GATK, v. 3.5-0) was then applied to realign local indels, recalibrate base scores, and identify point mutations and small insertions and deletions. Somatic point mutations and indels were called using MuTect2 by comparing tumor DNA to germline control and copy number estimation was obtained through modified ASCAT2 package.

Results

Patient Characteristics

From November 2015 to July 2017, 14 eligible mCRPC patients with detectable CTCs by CellSearch™ were enrolled (median age 70.4 years; range 60-77); time from PC diagnosis to procedure ranged from 2-11.6 years (mean: 6.2 years; median: 3.9 years). Median PSA level at apheresis was 506ng/mL (range: 41-6089 ng/mL); all 14 (100%) had metastatic bone disease. Prior to apheresis, patients had received 1-5 lines of systemic therapy for CRPC (**Supplementary Table 1, Supplementary Figure 1a)**. At apheresis, none of the subjects were receiving active treatment other than androgen deprivation.

The apheresis workflow is depicted in **Figure 1a**. Each apheresis procedure lasted between 90-160 minutes; apheresis product volume ranged from 40-100 mL (**Supplementary Table 2**). Apheresis was well tolerated with no related adverse events recorded during the procedure or in the 30-day follow-up. Neutrophil and lymphocyte counts did not change significantly following apheresis (**Supplementary Figure 1b)**.

CTC counts

The mean CTC count taken before and after apheresis was 167 and 193, per 7.5mLs of peripheral blood (PB), respectively. Surprisingly, the CTC count did not decrease

Downloaded from clincancerres.aacrjournals.org on April 24, 2019. © 2018 American Association for Cancer Research.

Author Manuscript Published OnlineFirst on August 9, 2018; DOI: 10.1158/1078-0432.CCR-18-0862
Author manuscripts have been peer reviewed and accepted for publication but have not yet been edited.

significantly following apheresis (p=0.48). The average inferred CTC harvest from an apheresis (mean volume = 59.5mL) was 12546, with apheresis yielding a 90-fold average increased yield. (p<0.001) (**Figure 1b and Supplementary Table 2**).

Single CTC genomic profiling

To validate the serial WGA and array CGH that we performed on single CTCs, we first used normal male and female DNA (aCGH verified by Agilent), as well as single white blood cell (WBC) amplified DNA, and showed that there was no bias amplifications or deletions. (**Supplementary Figure 2a and 2b**). Extracted single CTC DNA from a patient with known tumor biopsy CNAs was then evaluated, confirming robust CNA calling. WGA of 1µL of serially diluted samples (starting DNA templates: 10ng/µL, 1ng/µL, 0.1ng/µL and 0.03ng/µL) showed no amplification bias with consistent calling of gains and losses at all dilutions (**Supplementary Figure 2c**).

We then analyzed 205 single CTC aCGH genomic profiles for CNAs from the apheresis products of 14 patients with 185 CTC (90%) showing complex genomic copy change profiles and 20 (10%) cells having relatively flat genomic copy number profiles. Surprisingly, only 2 of the evaluated 14 patients had cell populations with both flat and cancer-like aCGH profiles suggesting that these sorted cells could be associated with specific tumor sub-types or induced by some treatments. We then aggregated the aCGH copy number profiles of all the individual CTCs and showed that the overall profile matched that previously reported for advanced PC whole biopsy exomes [18] (**Figure 1c**). Details for individual CTCs per patient are shown in Supplementary Table 3.

Tumor biopsies (treatment-naïve diagnostic biopsies and/or metastatic biopsies) were available for 12 of these 14 patients; these samples were also evaluated. Copy number traces of single CTCs and matching, same patient, biopsies showed broadly similar genomic profiles (**Figure 1c, Supplementary Figure 3)**, and again matched that of publically available data [18]. Differences were frequently observed between treatment-naïve biopsies and castration resistant CTCs including *AR* gain (X chromosome), *MYC* gain (8q) and *RB1* loss (chromosome 13) likely reflecting tumor evolution under treatment selective pressures (**Supplementary Figure 4**). High concordance between single CTC genomic profiles and contemporaneous, same patient, metastatic biopsies was seen, although intra-patient genomic heterogeneity was discernable from the single CTC analyses but not the bulk biopsy analyses.

Downloaded from clincancerres.aacrjournals.org on April 24, 2019. © 2018 American Association for Cancer Research.

Author Manuscript Published OnlineFirst on August 9, 2018; DOI: 10.1158/1078-0432.CCR-18-0862
Author manuscripts have been peer reviewed and accepted for publication but have not yet been edited.

CTC diversity

Overall, the genomic analyses of 185 single CTCs from 14 patients (**Figure 2a**) revealed that some patients had highly homogenous CTC CNA traces **(Figure 2a, left)** while others had highly diverse single CTC CNA traces **(Figure 2a, right)** with many lethal PCs displaying inter-cell heterogeneity. This may be related to disease phenotypes or acquired treatment resistance mechanisms (*AR* and *MYC* gain at chromosomes X and 8q respectively; *BRCA2/RB1* locus loss at chromosome 13). There was no significant correlation between median percentage genome alteration and intra-patient, inter-cell, diversity (**Figure 2b**) suggesting that this was due to true clonal diversity rather than aberration accumulation. Despite this, the unsupervised hierarchical clustering of all the CNA data from individual CTCs and same patient biopsies indicated that most samples from one patient clustered together (**Supplementary Figure 3**).

Intra-patient heterogeneity and tumor evolution

As depicted in **Figure 2a** (far left patients), the minority of patients had highly homogeneous CTC, including P09 (**Figure 3a)**; his contemporaneous mCRPC biopsy had a virtually identical CNA profile to these CTCs. Most evaluated patients had heterogeneous CTC CNA profiles that gross biopsy genomic analyses could fail to identify. To further interrogate this intra-patient heterogeneity, we studied additional cells in patient P13 who had heterogeneous CTCs, with CNA data suggesting distinct groups of cells (**Figure 3b**). Some CTCs clustered with his diagnostic prostatectomy sample, while others clustered with the mCRPC bone biopsy, with a breakpoint in the *PIK3R1* locus including most of chromosome 5q (**Figure 3c**). A third group of cells was also apparent, displaying more complex genomic aberrations.

FISH (fluorescence in-situ hybridization) analyses of the 5q21.1 locus was then performed on both the HSPC sample and the metastasis and revealed the presence of distinct copy number aberrant cells, with 5q21.1 being either gained, normal or lost in a mixed cell population. Overall, these analyses indicated that these three copy-states were equally common in the prostatectomy. Over time and following treatment, the proportion of tumor cells with 5q copy gain increased as shown in the mCRPC biopsy and apheresis CTCs and as confirmed by tissue FISH analyses (**Figures 3c and 3d).**

Downloaded from clincancerres.aacrjournals.org on April 24, 2019. © 2018 American Association for Cancer Research.

Author Manuscript Published OnlineFirst on August 9, 2018; DOI: 10.1158/1078-0432.CCR-18-0862
Author manuscripts have been peer reviewed and accepted for publication but have not yet been edited.

We then studied patient P03 since his CTC CNA profiles were also highly heterogeneous and multiple tumor samples taken at different time points were available, including a transurethral resection of the prostate (TURP) with four geographically and morphologically distinct regions (A, B, C, D) which were micro-dissected (**Figure 4a)**. aCGH genomic profiles of these regions identified intra-patient heterogeneity (**Figure 4b**). Homozygous deletion of *BRCA2* and 8q gain was present in all four regions; however, loss of chromosome 18 was only present in Areas C and D while gain of 7q was only present in Areas A and C. The CNA profile of a lymph node (LN) biopsy acquired from this patient 6 years later, following treatment with docetaxel, enzalutamide and cabazitaxel, identified the *BRCA2* homozygous deletion and 8q gain, as well as previously undetected *AR* amplification and 17q gain (**Figure 4b**).

In patient P03, we performed whole exome sequencing (WES) of the microdissected TURP regions. This identified truncal pathogenic mutations of SPOP (p.Trp131Cys) and FOXA1 (p.His168del), with intra-patient heterogeneity of other mutations indicating that regions A and C had similar mutation profiles when compared to regions B and D of the TURP, with the later LN biopsy WES identifying a mixture of these cell populations (**Figure 4c**). Single CTC analyses acquired at a later time point by apheresis also detected this heterogeneity, delineating this cancer's evolution as depicted by unsupervised hierarchal clustering of 13 CTCs, 4 micro-dissected TURP areas, the gross biopsy, and the LN biopsy (**Figure 4d and 4e)**. **Figure 4d** highlights key genomic differences in commonly altered pathways in these samples, with heterogeneous *PTEN* and *BRCA2* loss in different sub-clones. FISH analysis of TURP tissue using *MYC* and *BRCA2* probes revealed that some TURP tumor cells had concurrent *MYC* amplification and *BRCA2* homozygous deletion (**Figure 4f**), while others had *MYC* amplification but no *BRCA2* loss indicating that the latter was probably sub-clonal and occurred later, as indicated by the single CTC analyses (**Figure 4e).**

The apheresis from patient P05 also revealed heterogeneous CTCs; we successfully generated organoid cultures from these (**Supplementary Figure 5a and 5b**) utilizing previously described methods [19]. The CNA profile of these organoids clustered with this patient's CTCs with two genomically divergent sub-clones in culture (**Supplementary Figure 5c**) with both sub-clones detectable in the CTC analyses **(Supplementary Figure 5c, 5d)** indicating that CTC-derived organoid culture can recapitulate this diversity.

Conclusions/Discussion

Downloaded from clincancerres.aacrjournals.org on April 24, 2019. © 2018 American Association for Cancer Research.

Author Manuscript Published OnlineFirst on August 9, 2018; DOI: 10.1158/1078-0432.CCR-18-0862
Author manuscripts have been peer reviewed and accepted for publication but have not yet been edited.

Liquid biopsy by apheresis is non-invasive and well-tolerated, increasing CTC yield a hundred-fold from mCRPC patients. Apheresis did not significantly impact blood CTC counts suggesting constant replenishment or inefficient capture. Apheresis facilitated the interrogation of tumor genomics, inter-patient genomic heterogeneity, and the dissection of PC evolution. We show for the first time that the genomic landscape of PC CTCs captured by apheresis mirrors that of mCRPC biopsy exomes validating these CTC capture methods [18]. Copy number traces of individual CTCs frequently closely resembled same patient biopsies, with evidence for CTC CNAs evolving over time due to therapeutic pressures (including gains in *MYC* and *AR*). Critically, sub-clonal CNAs not easily discernable from bulk biopsy analyses were easily detected by single CTC analyses dissecting disease clonal evolution.

Yields of evaluable single cells decrease significantly through our experimental procedures; stringent settings in FACS sorting to allow isolation of only pure single cells results in a 60-80% retention rate of CTCs from CellSearch™ cartridges. DNA from approximately another 20% of these cells fail quality control after whole genome amplification. Therefore, in order to end up with sufficient CTCs for genomic analyses, a high number of cells are required, making the concentrated apheresis product a much more efficient source than peripheral blood.

Surprisingly, we identified by unsupervised clustering varying degrees of intra-patient heterogeneity with some patients having highly homogeneous single CTCs but most having intra-patient CTC genomic diversity. Some CTCs resembled diagnostic biopsies with others genomically mirroring metastases. We envision that the dynamic analyses of these clones by serial, repeated, apheresis before, during, and after treatment will not only dissect disease evolution but also help guide therapeutic switch decisions. Such heterogeneity remains difficult to identify from circulating free DNA, with the analyses of CTCs captured by apheresis allowing a more precise evaluation of emerging clones/sub-clones. Early identification of resistant clones can be utilized to reverse treatment failure, guiding drug combination administration or the serial utilization of drugs not tolerated when administered together. We propose that serial, multiple, apheresis procedures should now be embedded in drug trials to analyze tumor clones/sub-clone eradication/evolution during therapy to further evaluate this strategy while also generating estimates of CTC counts for monitoring response to therapy [20].

Downloaded from clincancerres.aacrjournals.org on April 24, 2019. © 2018 American Association for Cancer Research.

Author Manuscript Published OnlineFirst on August 9, 2018; DOI: 10.1158/1078-0432.CCR-18-0862
Author manuscripts have been peer reviewed and accepted for publication but have not yet been edited.

Further work is also now needed to explore the clinical implications of this diversity in intra-patient heterogeneity, evaluating whether distinct genomic subtypes of advanced PC display different levels of single CTC diversity. Moreover, further optimization of methodology generating successful organoid growth from apheresis products, along with subsequent molecular and functional analyses to confirm that these CTC-derived organoids can model mCRPC *ex vivo*, may also support the future study of drug testing in CTC organoid cultures.

We acknowledge the limitations of the data presented, particularly with regards to the limited cohort size and the fact that all the patients were treated at one tertiary cancer center making it difficult to draw broader clinical conclusions. In order for apheresis to have widespread utility it needs to be easily accessible, with high throughput CTC isolation from patients with other cancer types and with lower burden disease [21]. Moreover, improved methods to enhance CTC mobilization and yield through chemokine axis manipulation are warranted with such procedures potentially having therapeutic utility in patients with lower burden disease.

Moving forward, studies are needed to identify the optimal number of individual CTCs from one patient to sufficiently interrogate heterogeneity yet minimize cost. Low coverage whole genome next generation sequencing with barcoding of DNA from each CTC may allow this, as well as exploration of single cell RNA sequencing to better understand resistance mechanisms. Direct comparison of CTCs acquired by apheresis with both CTCs and cfDNA from peripheral blood, as well as with single cells dissociated from tissue should be pursued. Finally, studies to evaluate the large numbers of immune cells in the apheresis product from these patients are also merited.

In conclusion, we have demonstrated that the analyses of single CTCs captured by apheresis permits the identification of intra-patient tumor genomic heterogeneity previously missed by bulk biopsy analyses, providing previously undescribed detail on different mCRPC sub-clones. Although the study of biopsies remains a gold standard, the challenges of acquiring serial biopsies and disaggregating these to single cell suspensions to study disease evolution remain. We now posit that successfully and safely improving CTC yield for genomic analyses by apheresis is highly advantageous and has major potential implications for more precise cancer care.

Downloaded from clincancerres.aacrjournals.org on April 24, 2019. © 2018 American Association for Cancer Research.

Author Manuscript Published OnlineFirst on August 9, 2018; DOI: 10.1158/1078-0432.CCR-18-0862
Author manuscripts have been peer reviewed and accepted for publication but have not yet been edited.

Figure legends:

Figure 1. Overview of methodology, CTC counts and the overall genomic analyses: a) Methodology workflow of the study; **b)** CTC counts from 7.5mL of peripheral blood taken pre-apheresis, post-apheresis and compared to inferred harvested CTC counts in the total volume of apheresis product. **c)** The top plot represents the frequency of the genomic aberrations found in 185 single CTCs harvested by apheresis from 14 mCRPC patients; the middle plot represents the frequency of genomic aberrations from 150 mCRPC exomes (SU2C/PCF cohort), and the lower plot represents the frequency of genomic aberrations from available tissue biopsies from 12/14 patients. Chromosomes are shown across the x-axis whereas the y-axis represent the frequency of gains, losses, amplification and homozygous deletions. Gains are depicted in light pink, losses are depicted in light blue, amplification in dark red and homozygous/deep deletions are in dark blue. **aCGH of tissue biopsies were performed using female reference DNA (Agilent).*

Figure 2. Individual CTC CNA data depicting complex intra-patient and inter-patient genomic diversity: a) Unsupervised hierarchical clustering heatmap, based on Euclidean distance, of each analyzed individual CTC from each apheresis patient based on CTC CNA. Each patient is depicted with one color as shown on the phenobar at the top of the heatmap. The heatmaps of each individual patient are organized by their intra-patient diversity score from left to right. Chromosomal CNA are shown from top to bottom for each individual CTC; copy number gains are depicted in light blue, losses in pink, with amplifications and homozygous deletions in dark blue and dark red respectively. **b)** Box plot showing the percentage genome altered (%GA) for each of the patients. Each filled circle in the box plot represents the percentage genome altered of a single CTC.

Figure 3. Intra-patient CTC genomic heterogeneity. a) Individual CTC genome plots of patient P09 show very homogenous CTCs similar to a metastatic bone biopsy. **b)** Heat map depicting CNA of 23 CTCs (grey bars) and 2 tumor biopsies (black bars) from patient P13 showing two different sub-clones, readily visualized by focusing on chromosome 5q, and an additional group of highly heterogeneous CTCs (far left). **c)** FISH analysis of treatment naïve prostatectomy tissue and a bone mCRPC biopsy from patient P13 using probes for 5p11(red) and 5q21.1 (green). **d)** A schematic diagram showing the percentage of cells with copy number alterations on 5q21.1 with disease progression from the time of the prostatectomy until apheresis in patient P13.

Downloaded from clincancerres.aacrjournals.org on April 24, 2019. © 2018 American Association for Cancer Research.

Author Manuscript Published OnlineFirst on August 9, 2018; DOI: 10.1158/1078-0432.CCR-18-0862
Author manuscripts have been peer reviewed and accepted for publication but have not yet been edited.

Figure 4. Intra-patient genomic heterogeneity in patient P03: a) Tissue micrographs from four distinct TURP regions shown, depicting intra-patient heterogeneity of tumor morphology with A and C, as well as B and D, similar to one another. In regions A and C glandular differentiation is noticeable with small, monomorphic, hyperchromatic nuclei and inconspicuous nucleoli, whereas in regions B and D a more solid arrangement with pleomorphic nuclei and an open chromatin pattern with large, discernible nucleoli is seen. **b)** Genome profiles of these TURP regions presented by aCGH. Intra-patient heterogeneity between the 4 areas is highlighted by dashed red lines; regions A and C had gains of 17q and 12q and losses of 3p whereas regions B and D had loss of chromosome 18 and 2p. All areas had homozygous deletion of the *BRCA2* genomic locus. A metastatic lymph node biopsy taken at a later date had multiple new aberrations including new AR amplification. **c)** Exome sequencing revealed that while all samples had an SPOP mutation there was intra-patient heterogeneity as identified by morphology and copy number analysis. **d)** Heatmap depicting CNA heterogeneity for 12 selected prostate cancer genes with dendrogram utilizing hierarchical clustering of CNA data, based on Euclidean distance, for these tumor tissues and CTCs. Individual CTC are depicted as C#, with # depicting CTC number; “A” represents archival TURP material, “M” the metastatic lymph node biopsy, with A-A, A-B, A-C and A-D respectively representing TURP tissue from regions A, B, C and D respectively. **e)** Chromosome 13 plot showing heterogeneous *BRCA2* loss in different CTCs and biopsies. **f)** FISH analysis of TURP tumor tissue with *BRCA2* probe in green and *MYC* probe in red; *BRCA2* was homozygously deleted in most but not all cells (green arrows depict tumor cells with *BRCA2* heterozygous loss or no copy loss).

Downloaded from clincancerres.aacrjournals.org on April 24, 2019. © 2018 American Association for Cancer Research.

Author Manuscript Published OnlineFirst on August 9, 2018; DOI: 10.1158/1078-0432.CCR-18-0862
Author manuscripts have been peer reviewed and accepted for publication but have not yet been edited.

Supplementary Figure legends:

Supplementary Figure 1. Clinical data: a) Summary of prior treatments of all 14 patients prior to apheresis. **b)** A histogram presenting the lymphocyte and neutrophil counts ($x10^9$/L) in peripheral blood pre- and post-apheresis procedures.

Supplementary Figure 2. **Summary of the validation steps. a) Male vs female:** Genome plot of amplified male DNA vs amplified female DNA using the Ampli 1 kit. **b) WBC vs WBC:** Genomic profile of Ampli1 amplified WBCs against another WBC. **c) Dilution evaluation:** Genomic aberrations of an mCRPC sample with known CNA diluted serially to 10ng/µL, 1ng/µL, 0.1ng/µL, and 0.03ng/µL with all dilutions generating similar profiles after Ampli1^{TM} WGA and aCGH. Gains and amplification depicted in blue, and losses and homozygous/deep deletion in red.

Supplementary Figure 3. **Unsupervised clustering analyses of all samples:** Fan presentation of unsupervised clustering of all CTCs, tissue biopsies and organoids evaluated in this study. Each CTC is annotated as a circle, each tissue sample as a square, and an organoid as a triangle. Each apheresis patient is depicted by a color. CTCs largely cluster with tumor biopsies from the same patient although as a result of intrapatient heterogeneity some clustered away.

Supplementary Figure 4: Heatmaps presenting unsupervised hierarchical clustering based on CNA and Euclidean distance, of all the samples for each patient. Each individual patient is depicted by number from left to right, with chromosomal aberrations from top to bottom. Tumor biopsies are identified by black bars, and CTCs by green bars, at the bottom of the heatmap.

Supplementary Figure 5: Organoid cultures of CTCs acquired by apheresis from patient P05: a) Dendrogram and heat map of hierarchical clustering, based on Euclidean distance, for patient P05 evaluating CTC (green bars) and organoid CNAs (red). **b)** Micrographs of two organoids from P05 with scale bar in bottom left (100µm)**. c)** Phylogenetic tree showing the cultured organoids have CNA that cluster with CTCs. **d)** Two organoids and 3 CTCs with truncal CNA including shared *BRCA2* loss and *AR* amplification but sub-clonal chromosome 1 aberrations.

Supplementary Table legends

Supplementary Table 1: **Baseline characteristics of study patients (n=14).**

Downloaded from clincancerres.aacrjournals.org on April 24, 2019. © 2018 American Association for Cancer Research.

Author Manuscript Published OnlineFirst on August 9, 2018; DOI: 10.1158/1078-0432.CCR-18-0862
Author manuscripts have been peer reviewed and accepted for publication but have not yet been edited.

*All values given are at time of apheresis unless otherwise specified.

∧The Eastern Cooperative Oncology Group (ECOG) performance status score ranges from 0 to 5, with 0 indicating no symptoms and higher scores indicating increasing disability.

Supplementary Table 2: Summary of the CTC and WBC counts from both peripheral blood and apheresis product for all 14 patients, with additional clinical characteristics including sites of disease at apheresis and time to disease progression following apheresis procedure (when available). [ND = Not determined; WBC = White Blood Cells; CTC = Circulating Tumor Cells; PB = Peripheral Blood; Tot.Vol = Total Volume; Inc. = Increase]

Supplementary Table 3: Summary of individual CTCs per patient with percentage of the genome covered by a copy number segment and percentage of genes that are altered.

Downloaded from clincancerres.aacrjournals.org on April 24, 2019. © 2018 American Association for Cancer Research.

Author Manuscript Published OnlineFirst on August 9, 2018; DOI: 10.1158/1078-0432.CCR-18-0862
Author manuscripts have been peer reviewed and accepted for publication but have not yet been edited.

Authors' Contributions

Conception and design: MBK Lambros, LWMM Terstappen, Nikolas Stoecklein, J.S. de Bono.

Development of methodology: MBK Lambros, G Seed, S Sumanasuriya, V Gil, M Crespo, A Mackay, W Yuan, G Fowler, B Ebbs, P Flohr, S Miranda, RP Neves, K. Andree, J. Swennenhuis, LWMM Terstappen, NH Stoecklein and J.S. de Bono

Acquisition of data (provided animals, acquired and managed patients, provided facilities, etc.): MBK Lambros, G Seed, S Sumanasuriya, V Gil, M Crespo, A Mackay, M Fontes, G Fowler, B Ebbs, P Flohr, S Miranda, W Yuan, A Mackay, A Ferreira, R Pereira, C Bertan, I Figueiredo, R Riisnaes, D Nava Rodrigues, A Sharp, J Goodall, G Boysen, S Carreira, N Mehra, R Chandler, D Bianchini, P Rescigno, Z Zafeirou, J Hunt, D Moloney, L Hamilton and J.S. de Bono.

Analysis and interpretation of data (e.g., statistical analysis, biostatistics, computational analysis): MBK Lambros, G Seed, A Mackay, W Yuan, A Sharp and J.S. de Bono

Writing, review, and/or revision of the manuscript: MBK Lambros, S Sumanasuriya, M Crespo, V Gil, M Fontes, LWMM Terstappen and J.S. de Bono.

Administrative, technical, or material support (i.e., reporting or organizing data, constructing databases: MBK Lambros, G Seed, M Crespo, S Sumanasuriya, V Gil, and J.S. de Bono

Study supervision: J.S. de Bono

Other (member of trial management, oversight of trial conduct, and sample collection): S Sumanasuriya, A Sharp, N Mehra, R Chandler, D Bianchini, P Rescigno, Z Zafeirou, J Hunt, D Moloney, L Hamilton and J.S. de Bono.

Acknowledgements

We would like to acknowledge funding support from the following: FP7-HEALTH-2012-INNOVATION *(CTC-TRAP:EUFP7* grant #305341); Movember London Prostate Cancer Centre of Excellence (Movember/PCUK CEO13-2-002); Prostate Cancer Foundation (PCF grant 20131017); Prostate Cancer UK (PCUK PG12-49); Stand Up To Cancer–Prostate Cancer Foundation Prostate Dream Team Translational Cancer Research Grant (SU2C-AACR-DT0712; PCF grants 20131017 and 20131017-1); a Cancer Research UK Centre Programme grant; Experimental Cancer Medicine Centre grant funding from Cancer Research UK and the Department of Health; and Biomedical Research Centre funding to the Royal Marsden (ECMC CRM064X).

Downloaded from clincancerres.aacrjournals.org on April 24, 2019. © 2018 American Association for Cancer Research.

Author Manuscript Published OnlineFirst on August 9, 2018; DOI: 10.1158/1078-0432.CCR-18-0862
Author manuscripts have been peer reviewed and accepted for publication but have not yet been edited.

References

1. Siegel, R.L., K.D. Miller, and A. Jemal, *Cancer statistics, 2016.* CA Cancer J Clin, 2016. **66**(1): p. 7-30.
2. Attard, G., et al., *Improving the outcome of patients with castration-resistant prostate cancer through rational drug development.* Br J Cancer, 2006. **95**(7): p. 767-74.
3. Haffner, M.C., et al., *Tracking the clonal origin of lethal prostate cancer.* J Clin Invest, 2013. **123**(11): p. 4918-22.
4. Goodall, J., et al., *Circulating Cell-Free DNA to Guide Prostate Cancer Treatment with PARP Inhibition.* Cancer Discov, 2017. **7**(9): p. 1006-1017.
5. Wan, J.C.M., et al., *Liquid biopsies come of age: towards implementation of circulating tumor DNA.* Nat Rev Cancer, 2017. **17**(4): p. 223-238.
6. Premasekharan, G., et al., *An improved CTC isolation scheme for pairing with downstream genomics: Demonstrating clinical utility in metastatic prostate, lung and pancreatic cancer.* Cancer Lett, 2016. **380**(1): p. 144-52.
7. Cristofanilli, M., et al., *Circulating tumor cells, disease progression, and survival in metastatic breast cancer.* N Engl J Med, 2004. **351**(8): p. 781-91.
8. Lucci, A., et al., *Circulating tumor cells in non-metastatic breast cancer: a prospective study.* Lancet Oncol, 2012. **13**(7): p. 688-95.
9. de Bono, J.S., et al., *Circulating tumor cells predict survival benefit from treatment in metastatic castration-resistant prostate cancer.* Clin Cancer Res, 2008. **14**(19): p. 6302-9.
10. Kling, J., *Beyond counting tumor cells.* Nat Biotechnol, 2012. **30**(7): p. 578-80.
11. Budd, G.T., et al., *Circulating tumor cells versus imaging--predicting overall survival in metastatic breast cancer.* Clin Cancer Res, 2006. **12**(21): p. 6403-9.
12. Danila, D.C., et al., *Circulating tumor cell number and prognosis in progressive castration-resistant prostate cancer.* Clin Cancer Res, 2007. **13**(23): p. 7053-8.
13. Scher, H.I., et al., *Circulating tumor cell biomarker panel as an individual-level surrogate for survival in metastatic castration-resistant prostate cancer.* J Clin Oncol, 2015. **33**(12): p. 1348-55.
14. Stoecklein, N.H., et al., *Challenges for CTC-based liquid biopsies: low CTC frequency and diagnostic leukapheresis as a potential solution.* Expert Rev Mol Diagn, 2016. **16**(2): p. 147-64.
15. Bambauer, R., et al., *Therapeutic Apheresis in Hematologic, Autoimmune and Dermatologic Diseases With Immunologic Origin.* Ther Apher Dial, 2016. **20**(5): p. 433-452.

Downloaded from clincancerres.aacrjournals.org on April 24, 2019. © 2018 American Association for Cancer Research.

Author Manuscript Published OnlineFirst on August 9, 2018; DOI: 10.1158/1078-0432.CCR-18-0862
Author manuscripts have been peer reviewed and accepted for publication but have not yet been edited.

16. Sumanasuriya, S., M.B. Lambros, and J.S. de Bono, *Application of Liquid Biopsies in Cancer Targeted Therapy.* Clin Pharmacol Ther, 2017. **102**(5): p. 745-747.
17. Kiki C. Andree, A.M., Martin Scholz, Roland Kirchner, Rui P. Neves, Christiane Driemel, Rita Lampignano, Hans Neubauer, Dieter Niederacher, Tanja Fehm, Wolfram T. Knoefel, Johannes C. Fischer, Nikolas H. Stoecklein and Leon WMM Terstappen, *The isolation of CTC from diagnostic leukapheresis.* Cancer research, 2016. **Volume 76**(Issue 14): p. Supplement, pp. 1532.
18. Robinson, D., et al., *Integrative clinical genomics of advanced prostate cancer.* Cell, 2015. **161**(5): p. 1215-1228.
19. Gao, D., et al., *Organoid cultures derived from patients with advanced prostate cancer.* Cell, 2014. **159**(1): p. 176-187.
20. Armstrong, A.J., et al., *Biomarkers in the management and treatment of men with metastatic castration-resistant prostate cancer.* Eur Urol, 2012. **61**(3): p. 549-59.
21. Fischer, J.C., et al., *Diagnostic leukapheresis enables reliable detection of circulating tumor cells of nonmetastatic cancer patients.* Proc Natl Acad Sci U S A, 2013. **110**(41): p. 16580-5.
22. Punnoose, E.A., et al., *PTEN loss in circulating tumor cells correlates with PTEN loss in fresh tumor tissue from castration-resistant prostate cancer patients.* Br J Cancer, 2015. **113**(8): p. 1225-33.
23. Drost, J., et al., *Organoid culture systems for prostate epithelial and cancer tissue.* Nat Protoc, 2016. **11**(2): p. 347-58.

Downloaded from clincancerres.aacrjournals.org on April 24, 2019. © 2018 American Association for Cancer Research.

Figure 1

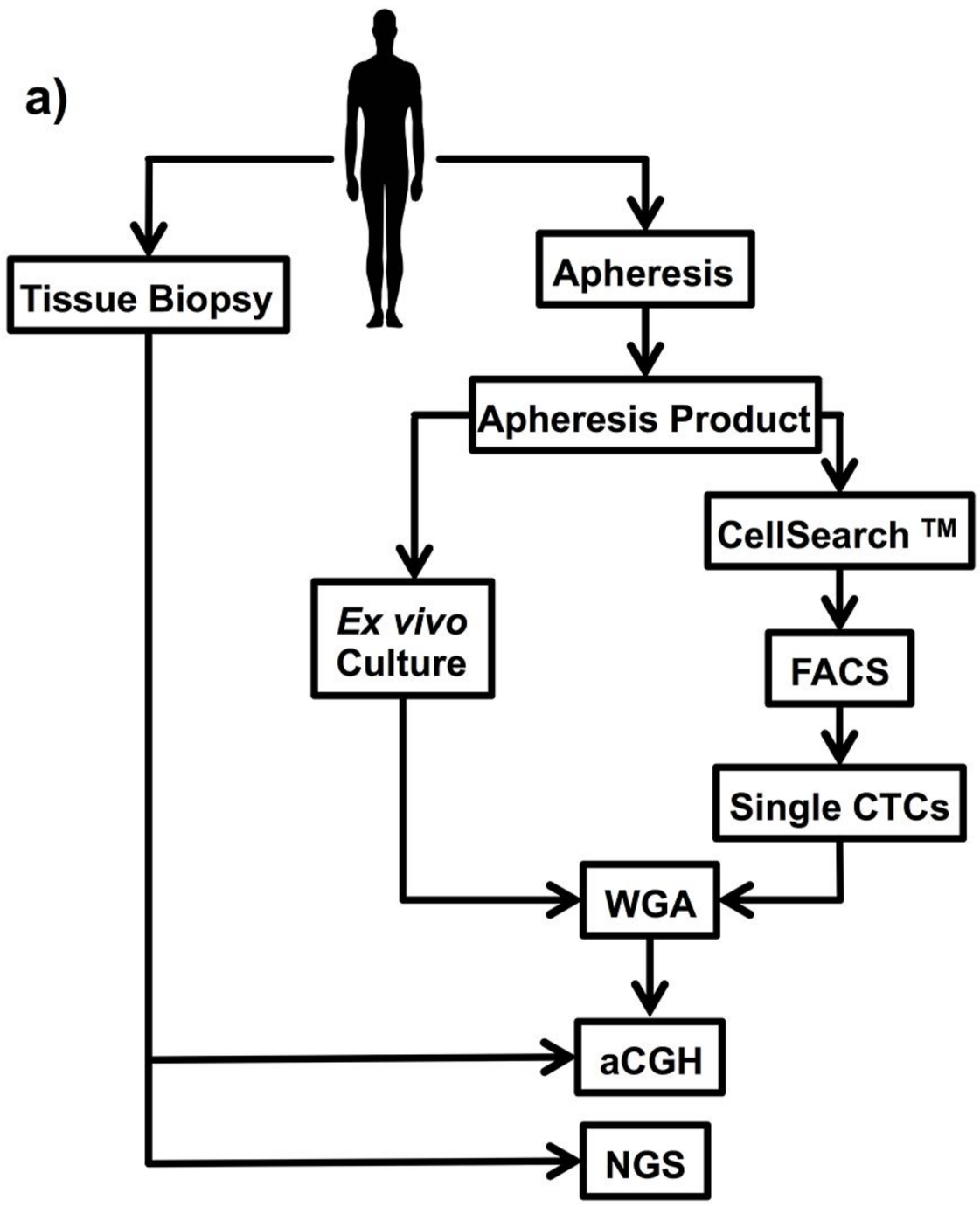

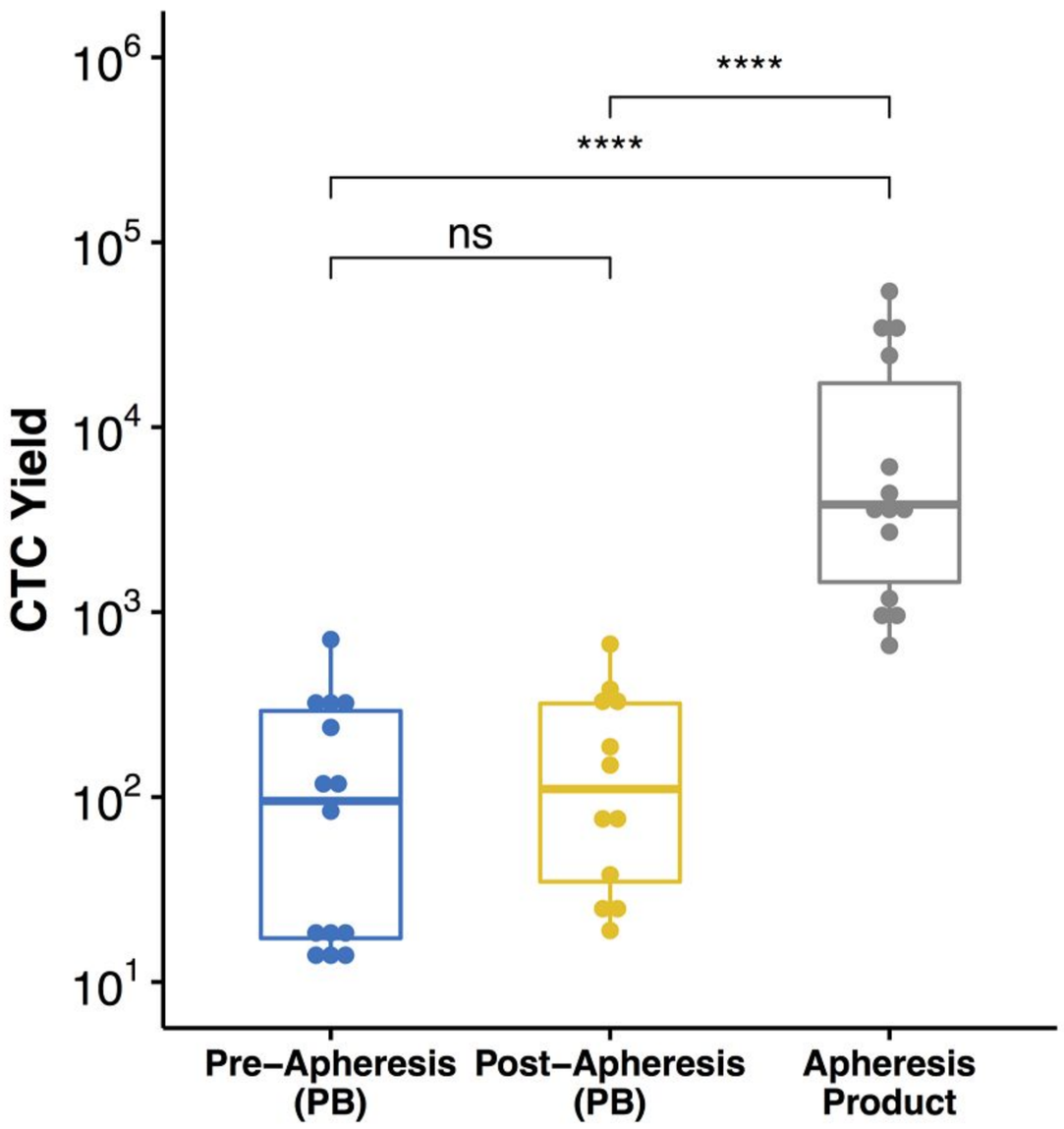

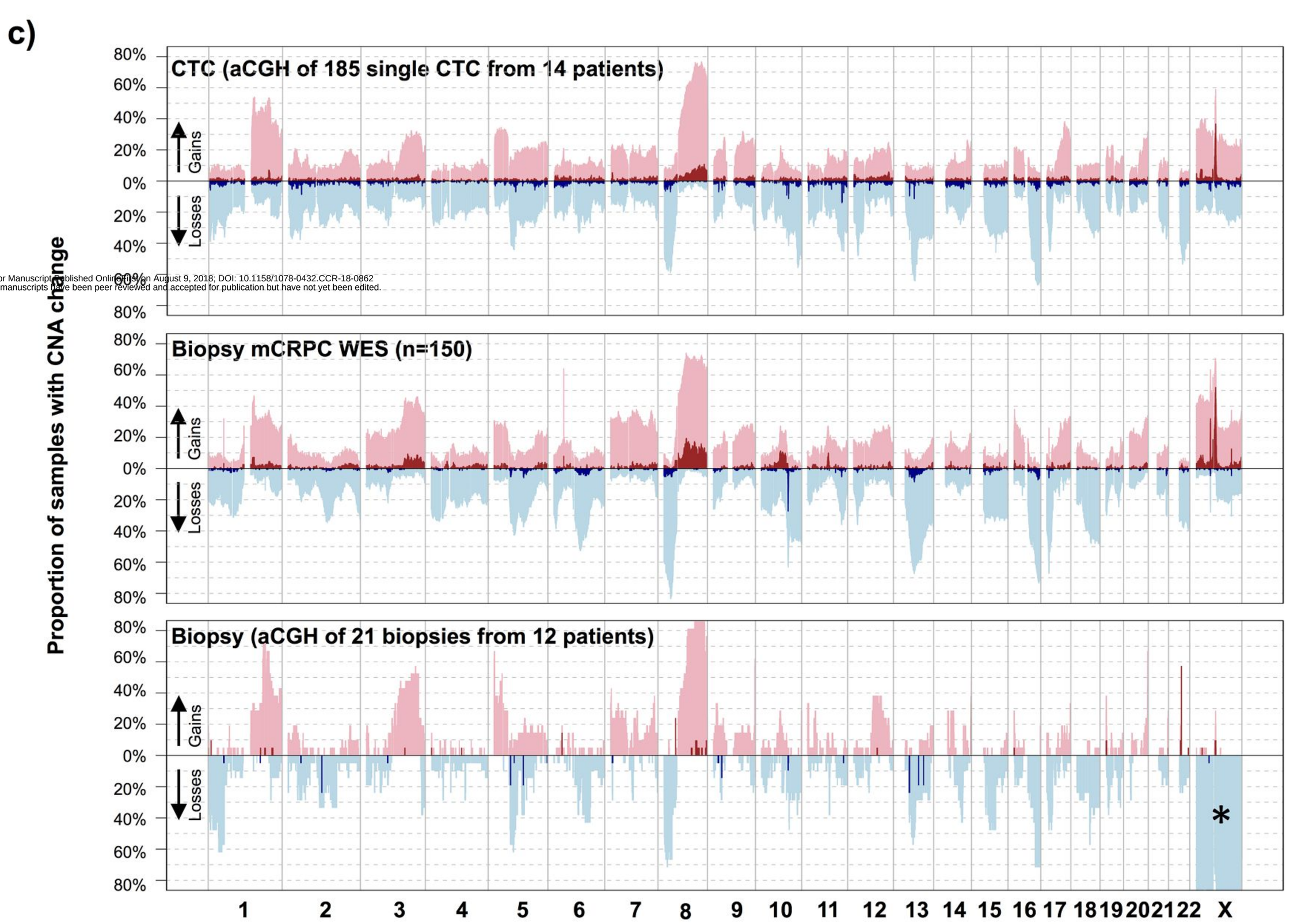

Author Manuscript Published OnlineFirst on August 9, 2018; DOI: 10.1158/1078-0432.CCR-18-0862
Author manuscripts have been peer reviewed and accepted for publication but have not yet been edited.

Downloaded from clincancerres.aacrjournals.org on April 24, 2019. © 2018 American Association for Cancer Research.

Figure 2

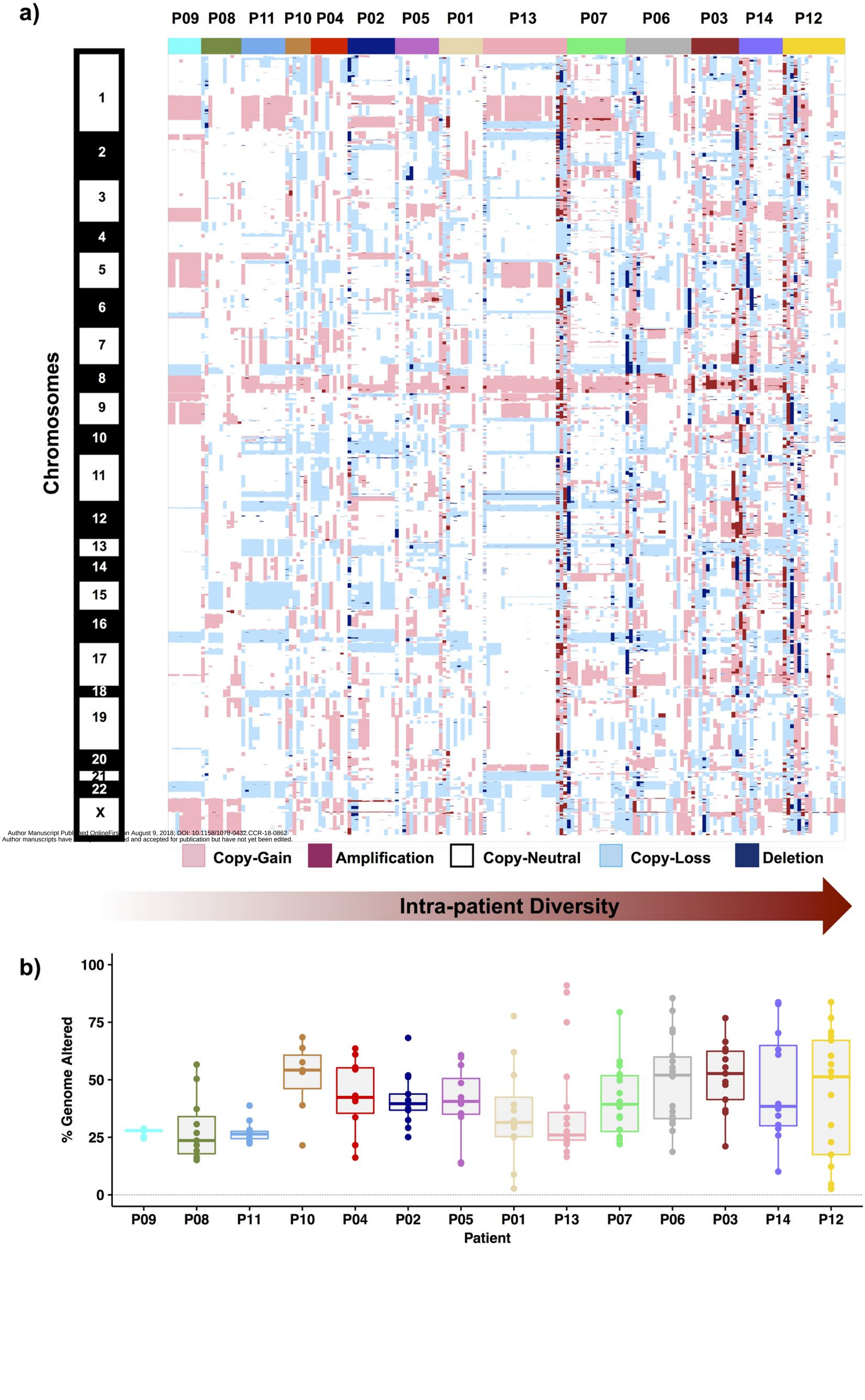

Author Manuscript Published OnlineFirst on August 9, 2018; DOI: 10.1158/1078-0432.CCR-18-0862
Author manuscripts have been peer reviewed and accepted for publication but have not yet been edited.

Downloaded from clincancerres.aacrjournals.org on April 24, 2019. © 2018 American Association for Cancer Research.

Figure 3

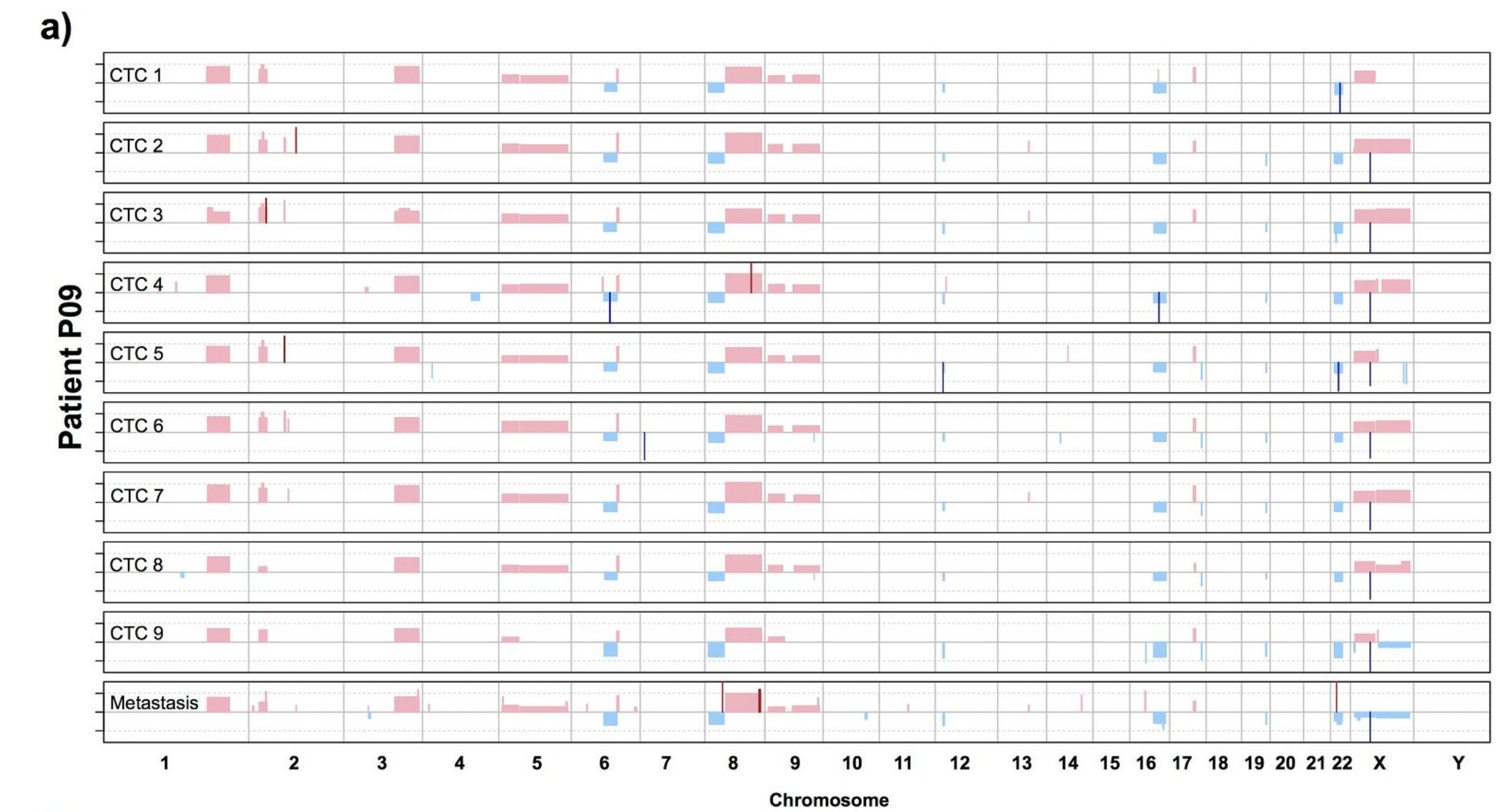

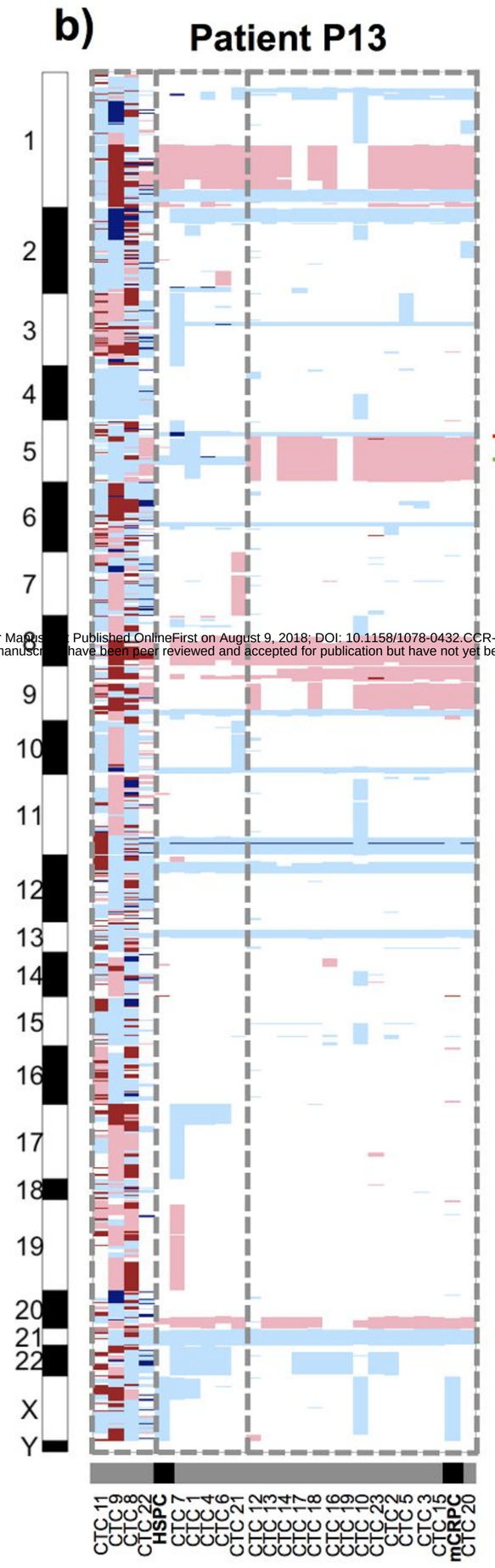

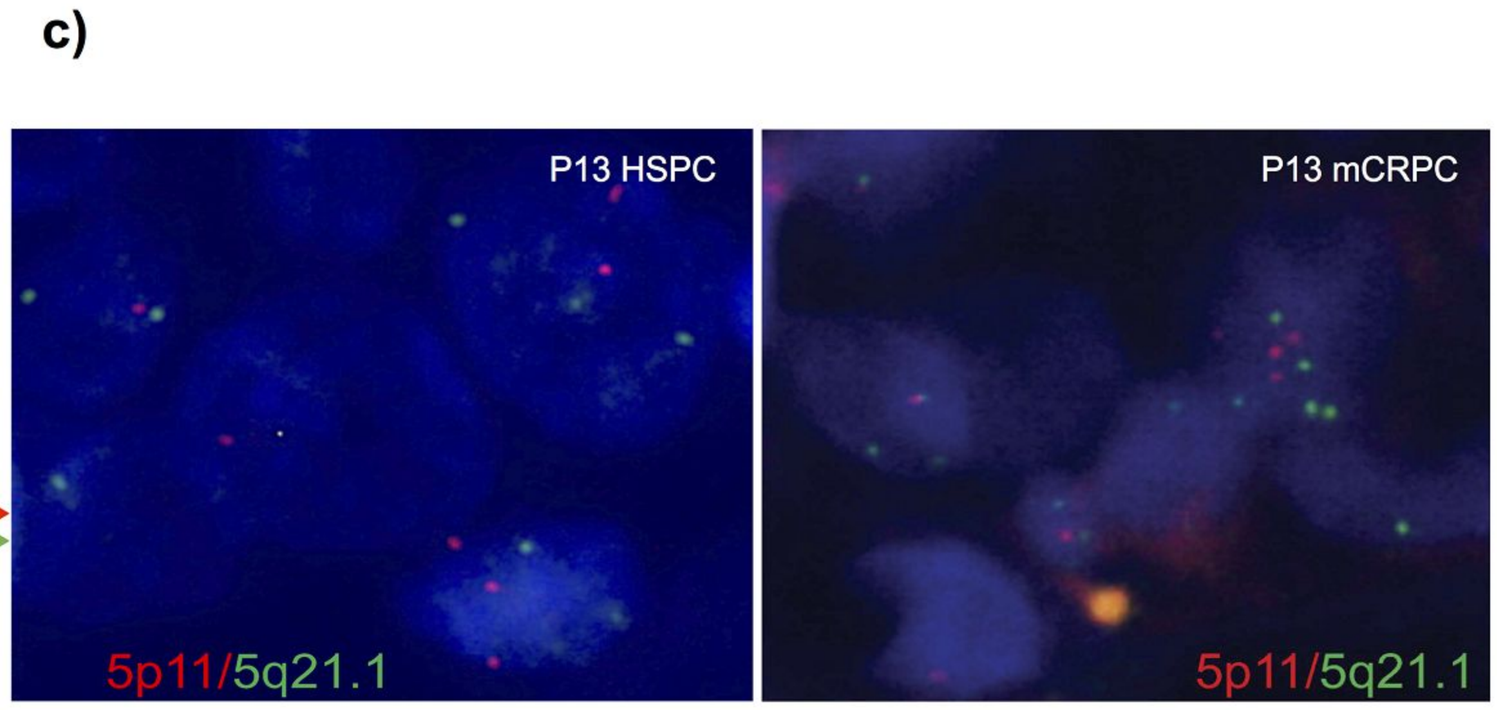

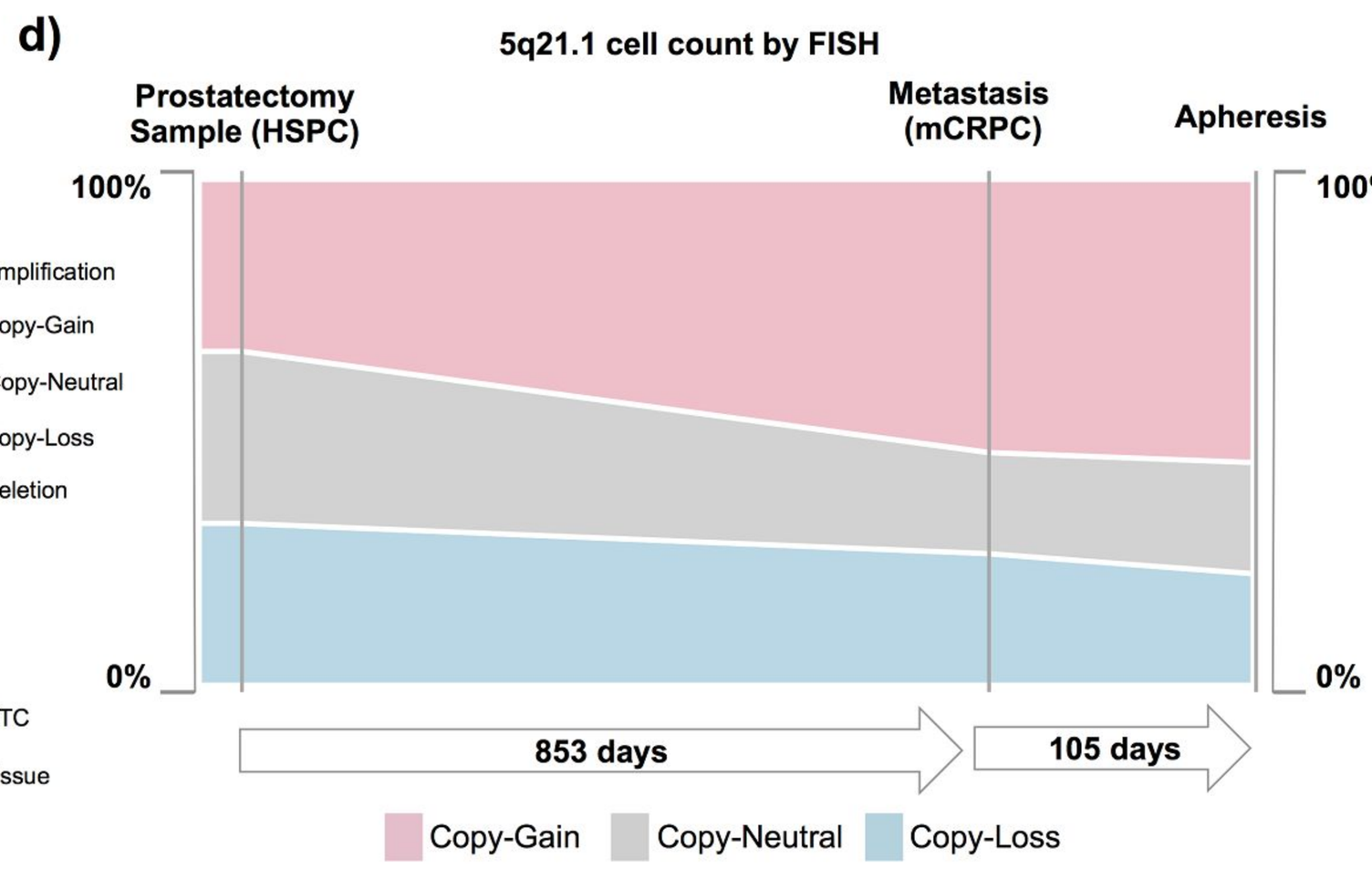

Author Manuscript Published OnlineFirst on August 9, 2018; DOI: 10.1158/1078-0432.CCR-18-0862
Author manuscripts have been peer reviewed and accepted for publication but have not yet been edited.

Downloaded from clincancerres.aacrjournals.org on April 24, 2019. © 2018 American Association for Cancer Research.

Figure 4

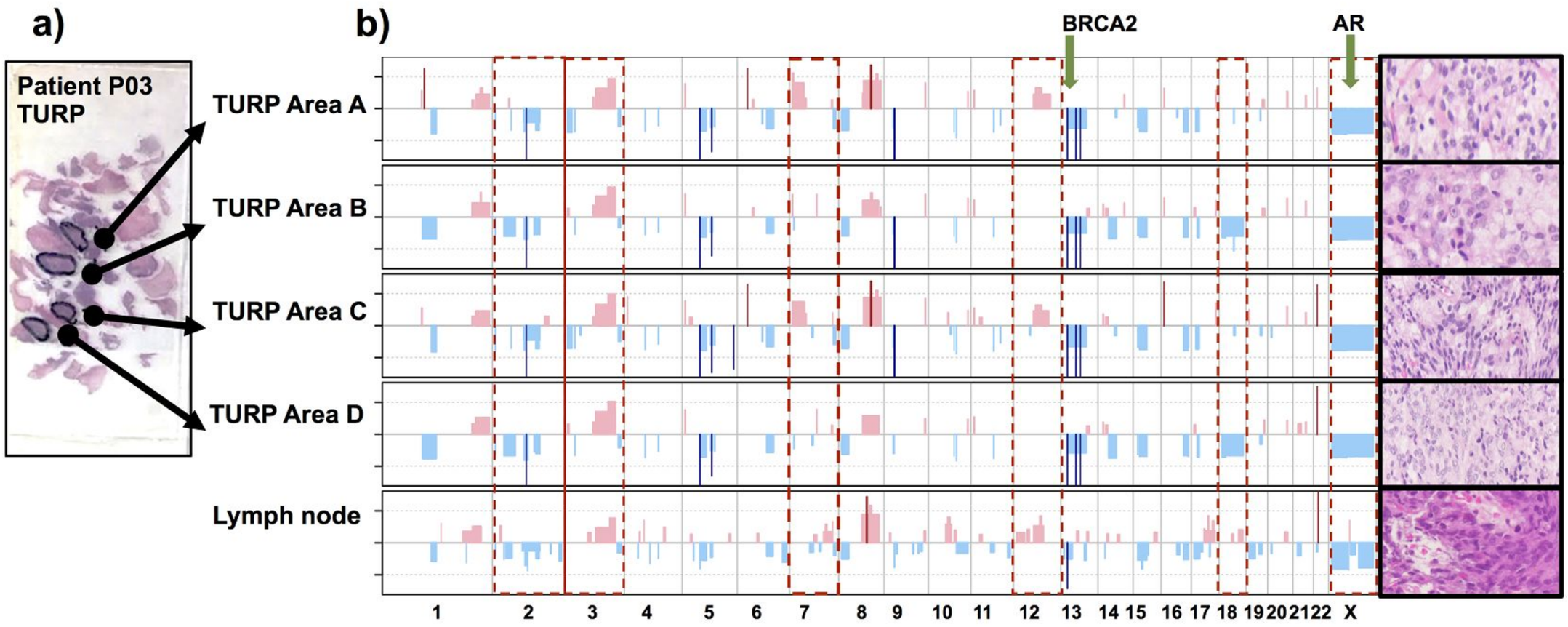

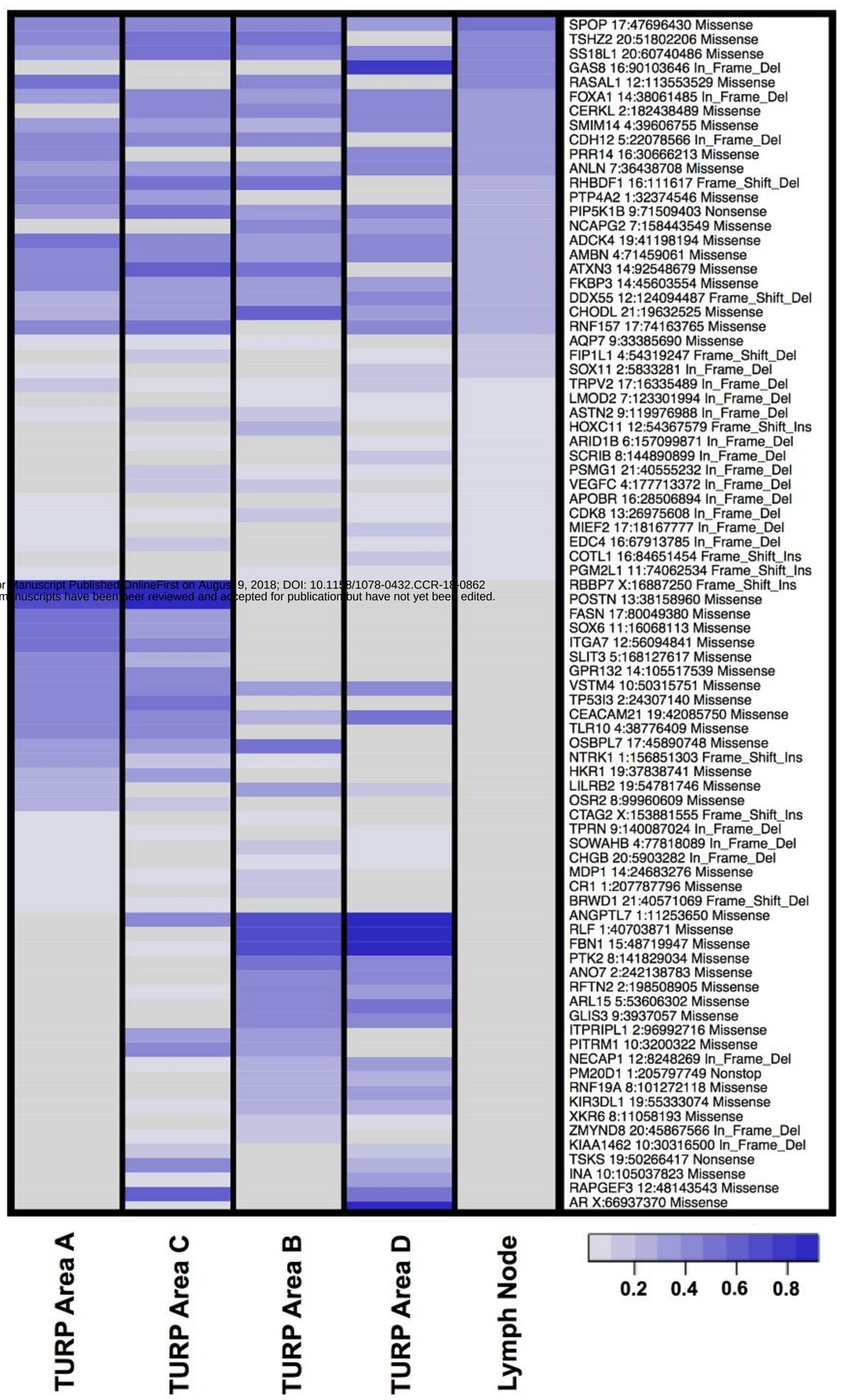

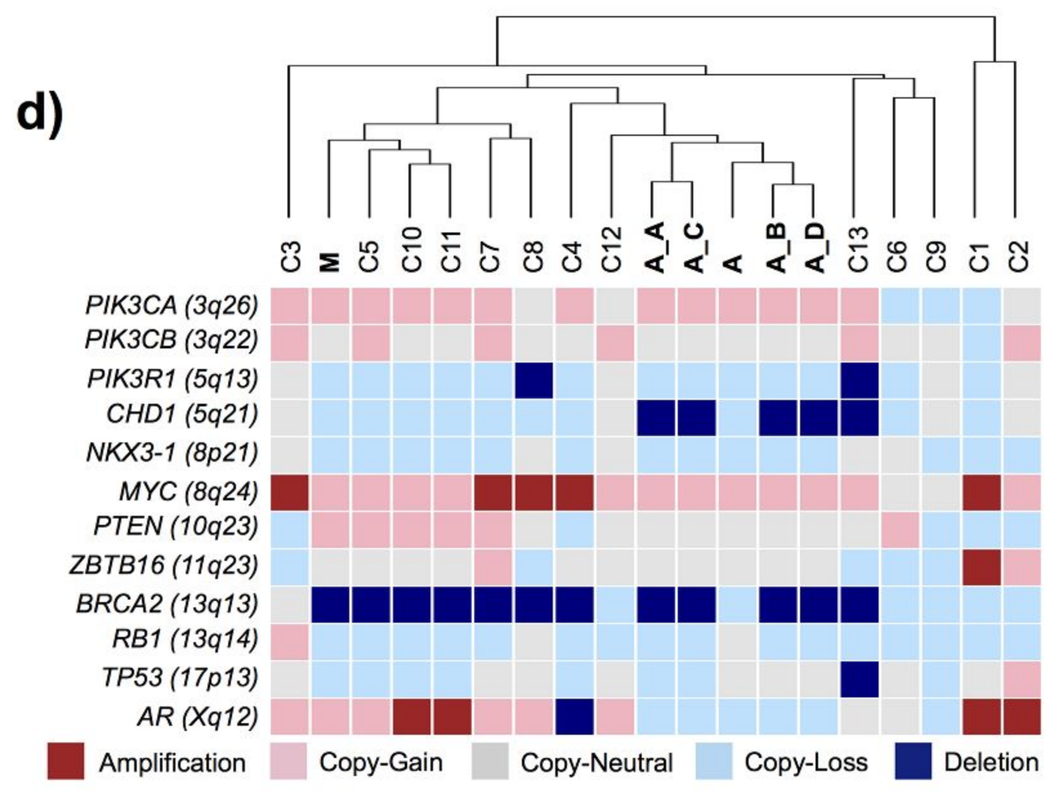

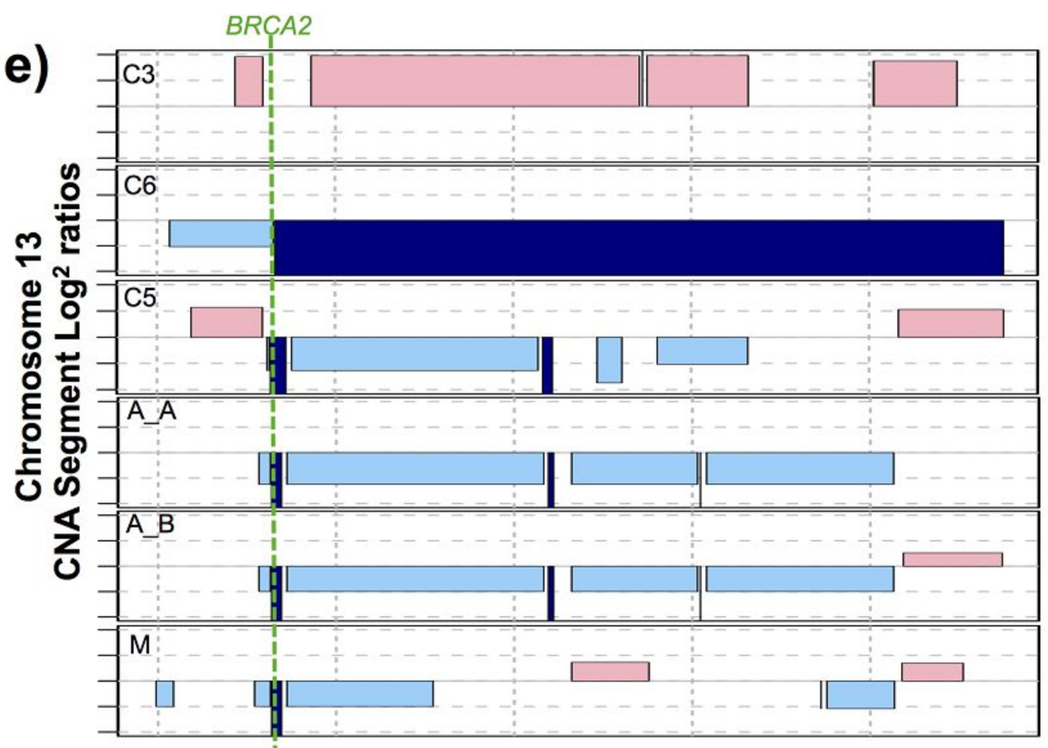

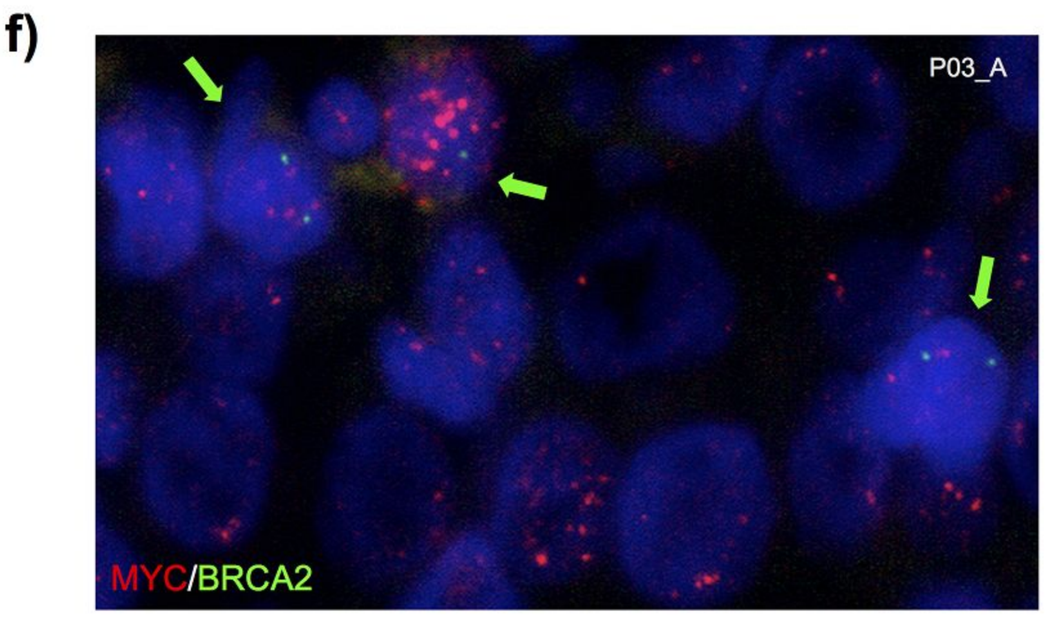

Author Manuscript Published OnlineFirst on August 9, 2018; DOI: 10.1158/1078-0432.CCR-18-0862
Author manuscripts have been peer reviewed and accepted for publication but have not yet been edited.

Downloaded from clincancerres.aacrjournals.org on April 24, 2019. © 2018 American Association for Cancer Research.

Author Manuscript Published OnlineFirst on August 9, 2018; DOI: 10.1158/1078-0432.CCR-18-0862
Author manuscripts have been peer reviewed and accepted for publication but have not yet been edited.

AACR American Association for Cancer Research

Clinical Cancer Research

Single Cell Analyses of Prostate Cancer Liquid Biopsies Acquired by Apheresis

Maryou BK Lambros, George Seed, Semini Sumanasuriya, et al.

Clin Cancer Res Published OnlineFirst August 9, 2018.

Updated version	Access the most recent version of this article at: doi:10.1158/1078-0432.CCR-18-0862
Supplementary Material	Access the most recent supplemental material at: http://clincancerres.aacrjournals.org/content/suppl/2018/08/09/1078-0432.CCR-18-0862.DC1
Author Manuscript	Author manuscripts have been peer reviewed and accepted for publication but have not yet been edited.

E-mail alerts	Sign up to receive free email-alerts related to this article or journal.
Reprints and Subscriptions	To order reprints of this article or to subscribe to the journal, contact the AACR Publications Department at pubs@aacr.org.
Permissions	To request permission to re-use all or part of this article, use this link http://clincancerres.aacrjournals.org/content/early/2018/08/08/1078-0432.CCR-18-0862. Click on "Request Permissions" which will take you to the Copyright Clearance Center's (CCC) Rightslink site.

Downloaded from clincancerres.aacrjournals.org on April 24, 2019. © 2018 American Association for Cancer Research.